

TANG HAI\*, LIU GUI-ZHONG\*\*, YAN YOU-BIN\*, GONG JIAN-LONG\*

## ENHANCEMENT OF REMOVAL OF ORGANIC POLLUTANTS FROM COKING WASTEWATER THROUGH ADSORPTION BY MODIFIED COAL FLY ASH

Potential use of modified coal fly ash (MCFA) has been investigated for adsorption of organic pollutants from coking wastewater (OPs-CW). The surface morphology, element profile, BET specific surface area and pore size distributions of MCFA were determined. FT-IR spectrum was used to detect changes of organic functional groups in MCFA after adsorption. The results showed that when the dosage of MCFA was 2.0 g/l at pH of 6.0, 94.2% of COD removal could be achieved after 600 min of agitation at 303 K. The adsorption kinetic of OPs-CW onto MCFA was fit well to the pseudo-second order model. The intraparticle diffusion was identified not to be a sole rate limiting step, and there may also be film diffusion. Freundlich model gave a better fit to all adsorption isotherms than Langmuir. The values of  $E_a$  calculated by D-R model are approximately in the range of 8–16 kJ/mol, suggesting that chemical bonding could be more likely to be the main adsorption mechanism. Negative values of  $\Delta G^\circ$  demonstrate feasibility and spontaneous nature of the adsorptive treatment.

### 1. INTRODUCTION

Coking wastewater is generated from coal coking, coal gas purification and by-product recovery processes of coking; it is refractory to treat by conventional biological processes [1] since it contains high concentrations of ammonia and toxic compounds such as phenols, cyanides, thiocyanate and PAHs [2]. Phenols have been included in priority-control pollutants by U.S. Environmental Protection Agency [3, 4], accounting for about 80% of the total COD. At present, coal is treated as one of the main energy sources in China; therefore recently Chinese government has imposed many stricter regulations to prevent discharge of toxic compounds from coking wastewater

---

\*School of Biochemical Engineering, Anhui Polytechnic University, Anhui, 241000, China; corresponding author Tang Hai, e-mail: newth76@163.com

\*\*Beijing Municipal Research Institute of Environmental Protection, Beijing, 100083, China.

into the environment. We found that various biological enhancement processes [5, 6] appear to be high performance technologies for advanced degradation of coking wastewater. However, the results of operation demonstrated that those processes could not fully satisfy the engineering needs for non-steady operation as well as high maintenance costs.

Adsorption has been shown to be a feasible alternative method for removing organic pollutants and heavy metals from wastewater. Several natural and synthetic hydrous solids have been investigated as adsorbents. Activated carbon is the most extensively employed but high costs of these materials limits their large scale use for removal. Thus, numerous approaches have been studied for the development of low cost adsorbents such as fly ash, peat, activated sludge, waste slurry and bio-sorbents. Fly ash is widely available as a waste product from electric power plants, which has been proven to be a suitable adsorbent for various pollutants [7–11].

We can see that adsorption of a large variety of single toxic chemical compounds by fly ash have received great attention. In this work, raw coal fly ash (RCFA) in its chemically modified form will be used to remove organic pollutants from coking wastewater (OPs-CW). However, to the best of the authors' knowledge, there were extremely few related reports in the open literature of OPs-CW adsorption onto modified coal fly ash (MCFA). Interest in this work will be on the investigation of the adsorption properties of MCFA for the treatment of coking wastewater. Physicochemical characterizations of MCFA such as surface morphology, elements profile, BET surface area, pore size distribution and various organic functional groups in MCFA were analyzed to better understand the mechanisms of OPs-CW adsorption onto MCFA. COD was used as the index for evaluating the treatment efficiency for OPs-CW since the compositions of coking wastewater were very complicated. The adsorption kinetics, adsorption equilibrium isotherms and thermodynamic parameters were studied.

## 2. MATERIALS AND METHODS

*Pretreatment and modification of MCFA.* Low grade pulverized RCFA was obtained from the firepower plant located in Shan Dong province (China); Its main components are as follows (in wt. %):  $\text{SiO}_2$  – 51.94%;  $\text{Fe}_2\text{O}_3$  – 13.10%;  $\text{Al}_2\text{O}_3$  – 24.06%;  $\text{CaO}$  – 3.74%;  $\text{MgO}$  – 0.93%;  $\text{TiO}_2$  – 0.96%;  $\text{SO}_3$  – 3.00%;  $\text{K}_2\text{O}$  – 1.52%;  $\text{Na}_2\text{O}$  – 0.32%;  $\text{P}_2\text{O}_5$  – 0.09%; and lost on ignition – 14.97%. The RCFA was firstly screened by 400 mesh sieve (37  $\mu\text{m}$ ), dried at 110 °C for 24 h, and immersed in 1.0 M HCl at 45 °C for 24 h. Then, the mixture was filtered, washed by large amounts of distilled water, and dried at 110 °C for 24 h. The dry mass was grinded to particle size ranging from 10 to 20  $\mu\text{m}$  and kept in a dry and clean place for use as MCFA.

*Raw wastewater.* The coking wastewater was obtained from the coking wastewater treatment plant located in Anhui province in China. Its color is dark red with a certain level of turbidity. It was characterized by the following relevant parameters: pH = 7.2; COD<sub>cr</sub> – 2845 mg/l; NH<sub>4</sub>-N – 268 mg/l; TN – 351 mg/l; volatile phenols – 586 mg/l; cyanides – 14 mg/l; SS – 520 mg/l; oil and grease – 45 mg/l; color – 1650°.

*Reagents and methods of analyses.* All reagents used in this work were analytical reagent grade and without any further purification. Distilled water was used for preparing all of the solutions and reagents. The initial pH (pH<sub>i</sub>) was adjusted with 0.1 M HCl or 0.1 M NaOH. COD was determined according to the standard methods for the examination of water and wastewater [12]. The pH value was measured with a pH meter (PHB-5, Shanghai Leici, China).

The surface morphologies and elements profile of RCFA and MCFA were observed with a scanning electron microscope with energy dispersive spectrum analysis (SEM/EDS) (S4800, Japan). The BET specific surface area ranging from 0.1–3500 m<sup>2</sup>/g and pore size distribution in the range of 2–200 nm were determined by an automated gas sorption system (NOVA 2000e, America), using N<sub>2</sub> as adsorbate at 77.35 K. The zeta potential was examined using a zeta meter (Coulter DELSA 440, Beckman, USA). The identification of organic functional groups in MCFA were performed using an FT-IR (IRPrestige-21, Japan) in the transmission mode at the resolution of 4 cm<sup>-1</sup> with the scanning in range of 4400–450 cm<sup>-1</sup>.

*Experimental procedure.* A known amount of MCFA was introduced into a 100 ml stoppered conical flask in which 100 ml of coking wastewater of known COD and pH<sub>i</sub> was already present. This mixture was kept in a temperature-controlled shaker at a constant speed of 150 rpm at a pre-decided constant temperature (*T*) for a certain contact time (*t*) to attain the desired adsorption stage. Then MCFA was separated from the mixture by ultracentrifugation and the wastewater was analyzed for COD or final pH (pH<sub>f</sub>) immediately.

For dosage and pH experiments, the percent COD removal was calculated using the following relationship:

$$\text{COD removal} = \frac{(C_0 - C_e)}{C_0} \times 100\% \quad (1)$$

where, *C*<sub>0</sub> and *C*<sub>*e*</sub> (mg/l) are the initial and equilibrium liquid phase COD, respectively.

Adsorption equilibrium experiments were carried out at the optimum pH<sub>i</sub> at temperatures from 303 to 333 K. The optimum dosage of MCFA was thoroughly mixed with coking wastewater for different initial values of COD. The amount of COD adsorbed at equilibrium onto MCFA, *q*<sub>*e*</sub> (mg/g), was calculated by the following mass balance relationship:

$$q_e = \frac{(C_0 - C_e)V}{W} \quad (2)$$

where  $V$  is volume of the mixture (l),  $W$  is the weight of MCFA used (g).

Adsorption kinetic studies were conducted at the optimum  $\text{pH}_i$  at 303 K. The optimum dosage of MCFA was thoroughly mixed individually with coking wastewater for different initial values of COD and samples were collected at required time intervals viz. 10–600 min. All the experiments were duplicated and only the mean values are reported. The maximum deviation observed was less than  $\pm 4\%$ .

*Adsorption theory.* The kinetics of OPs-CW adsorption onto MCFA was analyzed by using pseudo-first order, pseudo-second order and intraparticle diffusion models (Weber and Morris [13] and Dumwald–Wagner [14]):

- pseudo-first order model

$$\lg(q_e - q_t) = \lg q_e - k_1 t \quad (3)$$

- pseudo-second order model

$$\frac{t}{q_t} = \frac{1}{k_2 q_e^2} + \frac{t}{q_e} \quad (4)$$

- Weber and Morris model

$$q_t = K_{\text{dif}} t^{0.5} + C \quad (5)$$

Dumwald–Wagner model

$$B_t = -0.498 - \ln(1 - F) \quad (6)$$

where  $q_e$  and  $q_t$  are the adsorption capacities at equilibrium and after time  $t$ , respectively (mg/g),  $k_1$  and  $k_2$  are the rate constants of pseudo-first order (l/min) and pseudo-second order adsorption (g/(mg·min)), respectively,  $K_{\text{dif}}$  is the rate constant of the Weber and Morris model (mg/(g·min<sup>-0.5</sup>),  $C$  (mg/g) is the intercept of Eqs. (5).  $F = q_t/q_e$  is the fractional attainment of equilibrium at time  $t$ , and  $B_t$  is a mathematical function of  $F$ .

The Langmuir and Freundlich isotherms and D-R model [15] are expressed as:

- Langmuir isotherm

$$\frac{C_e}{q_e} = \frac{C_e}{q_o} + \frac{1}{q_o K_L} \quad (7)$$

- Freundlich isotherm

$$\lg q_e = \lg K_F + \frac{1}{n} \lg C_e \quad (8)$$

- D-R model

$$\ln q_e = \ln X'_m - K' \varepsilon^2 \quad (9)$$

$$\varepsilon = RT \ln \left( 1 + \frac{1}{C_e} \right) \quad (10)$$

$$E_a = \frac{1}{\sqrt{2K'}} \quad (11)$$

where  $C_e$  is the equilibrium COD (mg/l),  $q_e$  is the amount of COD adsorbed per unit of MCFA (mg/g),  $q_o$  is a constant related to the area occupied by a monolayer of adsorbate (mg/g),  $K_L$  is a direct measure of the intensity of the adsorption process (l/mg),  $k_F$  is the quantity of adsorbate in adsorbent for a unit equilibrium concentration (mg/g),  $K'$  is a constant related to the adsorption energy ( $\text{mol}^2/(\text{kJ}^2)$ ),  $X'_m$  is the theoretical saturation capacity (mg/g),  $\varepsilon$  is the Polanyi potential,  $E_a$  is the mean free energy (kJ/mol).

Thermodynamic parameters, including changes of: Gibbs free energy ( $\Delta G^\circ$ , kJ/mol), enthalpy ( $\Delta H^\circ$ , kJ/mol,) and entropy ( $\Delta S^\circ$ , J/(mol·K)) were used to check whether the adsorption process was spontaneous. The values of  $\Delta G^\circ$ ,  $\Delta H^\circ$  and  $\Delta S^\circ$  were calculated using the following equations [16]:

$$\Delta G^\circ = -RT \ln K_d \quad (12)$$

$$\Delta G^\circ = \Delta H^\circ - T\Delta S^\circ \quad (13)$$

where  $R$  is the gas constant (J/(mol·K)),  $T$  is temperature (K),  $K_d$  is the distribution coefficient.

### 3. RESULTS AND DISCUSSION

#### 3.1. CHARACTERIZATION OF ADSORBENTS

Figure 1 illustrates the SEM photographs of adsorbents. The morphologies at lower magnification (4000× or 5000×) show no significant differences, however some larger differences at higher magnification (18000×) on the surface texture between RCFA and MCFA can be observed. The surface of MCFA was rough and uneven and RCFA seemed flat and smooth. MCFA displayed porous structures with pores of varying sizes, and furthermore, numbers of pores observed in the RCFA are far lower than that in the MCFA. Figure 2 shows profiles of surface elements of RCFA and MCFA by using the normalization processing. It shows that the weight percentage are: 5.74%, 2.93% of iron (Fe), 13.08%, 10.08% of aluminum (Al) and 18.12%, 14.05% of silica

(Si) in RCFA and MCFA, respectively. It is obvious that RCFA contains higher amounts of Fe and Al with respect to MCFA. The differences may be due to the fact that the aluminum and iron was leached under hot strong acidity conditions, so as to cause the rapid formation of pore channel structure and an improve pore size of MCFA.

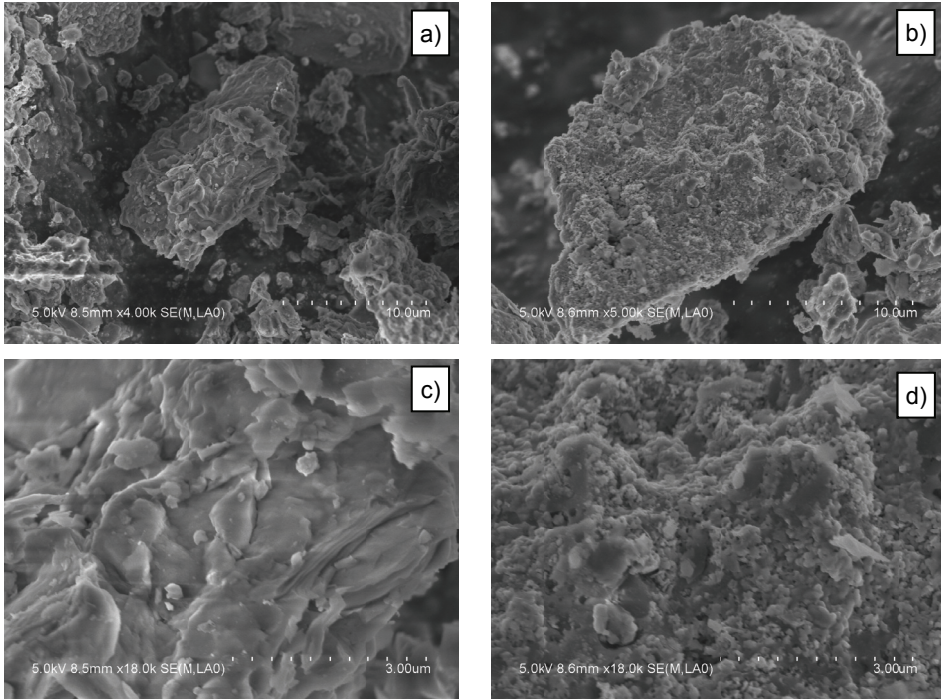


Fig. 1. SEM photographs of RCFA and MCFA:  
a) RCFA, 4000×, b) MCFA, 5000×, c) RCFA, 18 000×, d) MCFA 18 000×

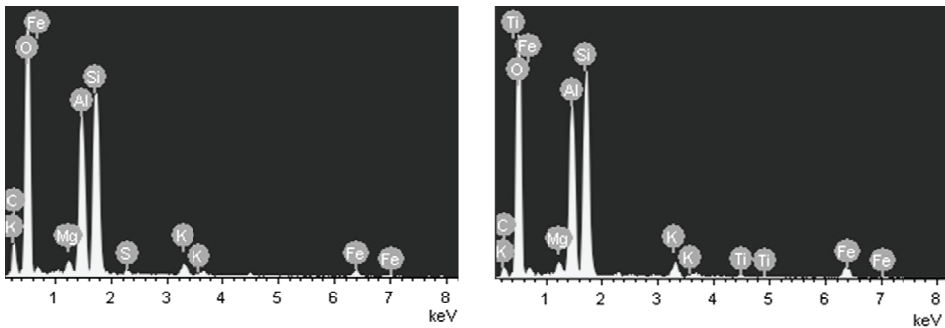


Fig. 2. Surface elements profile of RCFA (a) and MCFA (b)

The BET specific surface area ( $S_f$ , BET model [17]), pore volume ( $V_p$ ) and average pore diameter ( $D_{av}$ ) (BJH model [18]) of RCFA and MCFA measured with a NOVA 2000e automated system are listed in Table 1. The pore size distribution curve of MCFA and RCFA is shown in Fig. 3. Modification of RCFA can effectively increase specific surface area and total pore volumes of approximately 164% and 45%, respectively. Average pore diameter was decreased relatively. Furthermore, it was found that mesoporosity volume (2–50 nm [19]) exhibited a high percentage of total pore volume by the BJH pore size distribution desorption data curve.

Table 1  
Physical characterization of RCFA and MCFA

Speciation	RCFA	MCFA
$S_f$ [ $\text{m}^2/\text{g}$ ]	11.449	30.295
$V_p$ [ $\text{cm}^3/\text{g}$ ]	0.020	0.029
$D_{av}$ [nm]	3.746	3.701

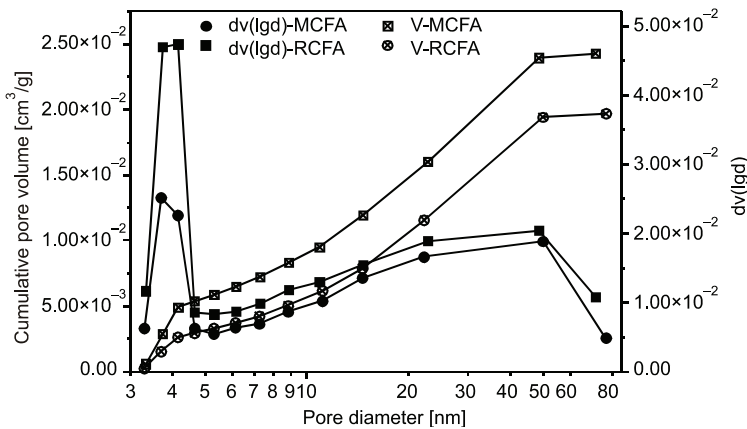


Fig. 3. Pore size distribution of RCFA and MCFA

### 3.2. EFFECT OF MCFA DOSAGE

Figure 4 shows the effect of MCFA dosage ranging from 0.15 to 7.5 g/l on percent COD removal at an initial COD concentration of 2845 mg/l at pH of 7.0 with adsorption equilibrium time of 10 h. The results showed that the removal efficiency increased quickly from 28.5% to 91.8% when the dosage of MCFA was increased from 0.15 to 2.0 g/l, and thereafter it remained almost constant while the dosage of MCFA increased from 2.0 to 7.5 g/l. This is due to the fact that the removal efficiency more depends upon the concentration of the solution and less depends upon the dose if it is larger than optimum dosage. Hence, the optimum MCFA dosage for OPs-CW removal was determined as a 2.0 g/l.

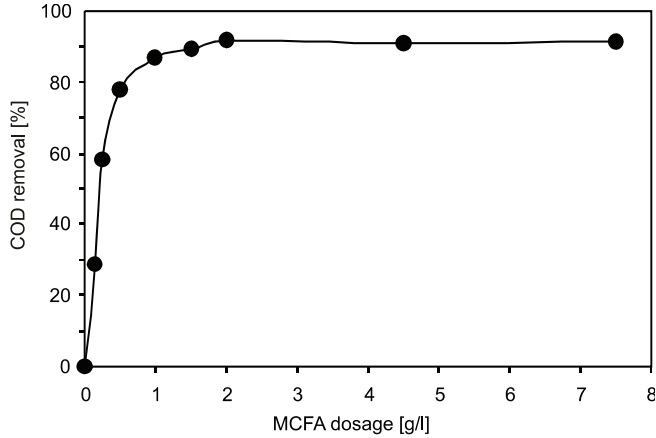


Fig. 4. Effect of MCFA dosage on OPs-CW adsorption onto MCFA ( $T = 303 \text{ K}$ ,  $t = 10 \text{ h}$ ,  $C_0 = 2845 \text{ mg/l}$ ,  $\text{pH} = 7.0$ )

### 3.3. EFFECT OF SOLUTION PH

The pH of adsorption medium is the most important parameter influencing the adsorption capacity because it relates to the adsorption mechanism onto the adsorbent surface and reflects the nature of the physicochemical interaction of the species in solution and the adsorptive sites of adsorbents. pH experiments were carried out at pH ranging from 3.0 to 10.0. It can be seen from Fig. 5 that the percent COD removal decreased from 94.2% to 47.3% when the pH was increased from 6.0 to 10.0.

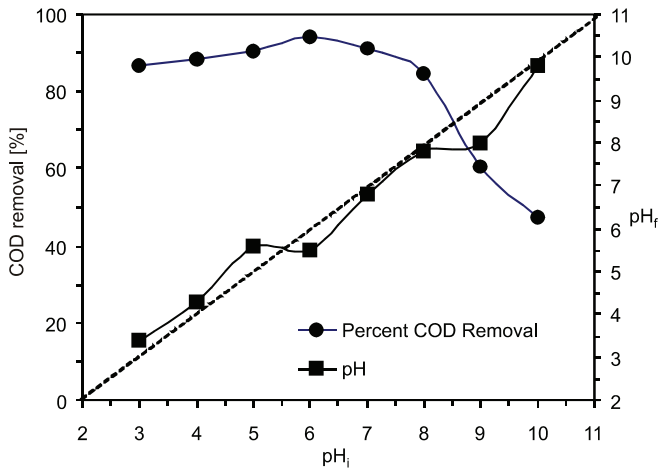


Fig. 5. Effect of initial pH on the OPs-CW adsorption by MCFA ( $T = 303 \text{ K}$ , contact time – 12 h,  $C_0 = 2845 \text{ mg/l}$ , MCFA dosage = 2.0 g/l)

This phenomenon can be explained that phenols and other OPs-CW will be easily adsorbed at MCFA compared with ionic states for its high hydrophobicity when non-ionic phenols predominate in the solution when the pH is far lower than 9.96 (isoelectric point of phenol,  $pK_a = 9.96$ ). However the optimum adsorption capacity was observed at pH of 6.0 rather than at 3.0–5.0. This suggested that the molecular adsorption was not the sole mechanism, revealing the fact that there exists electrostatic attraction mechanism of negatively charged functional groups from phenols and other OPs-CW due to the  $H^+$  ions and other cations located on the reactive sites of MCFA. Zeta  $\zeta$  potential analysis indicated that MCFA particles were positively charged in acidic solution with the  $\zeta$  potential of about 34 mV at pH 6.0. Similar observations have been reported by other workers for adsorption of reactive dyes indicating that the fly ash has a net positive charge on its surface [20]. Nevertheless, other factors may be occurrence of the MCFA disintegration (dissolving), it is needed to be studied further for complicated components of MCFA and coking wastewater. For pH, some experiments ( $pH_i < 6.0$ ), the  $pH_f$  values are higher than  $pH_i$ . It may be observed that as the  $pH_f$  values increase, the COD removal efficiency decreases. Therefore, pH of 6.0 is selected in the subsequent experiments.

#### 3.4. KINETICS OF ADSORPTION

Studies of adsorption kinetics were conducted at the initial COD concentration ranging from 2845 mg/l to 711 mg/l at 303 K. The effect of the initial COD and contact time on  $q_t$  is shown in Fig. 6a. It was evident that very rapid uptake can be achieved during first 150 min. The minimum contact time of 600 min can be assumed to be equilibrium time for the adsorption in all cases. The adsorption capacities at adsorption equilibrium are 130.5 mg/g, 63.6 mg/g and 31.67 mg/g at the initial COD of 2845 mg/l, 1422 mg/l and 711 mg/l, respectively. The regression constants for pseudo-first order, pseudo-second order and intraparticle diffusion model are listed in Tables 2 and 3. It can be seen from Table 2 that the correlation coefficient  $R^2$  is relatively lower than the pseudo-second order adsorption data, which shows that OPs-CW adsorption onto MCFA cannot be applied and the reaction mechanism is not a pseudo-first order reaction. Figure 6b shows the pseudo-first order equation. We found that it fits well for the first 150 min and thereafter the data deviate hardly from theory. The  $R^2$  values for the pseudo-second order kinetic model are higher than 0.999 which led to believe that the pseudo-second order kinetic model provided good correlation for the adsorption. Furthermore, in pseudo-second order kinetic model the calculated  $q_{e(cal)}$  are very close to experimental  $q_{e(exp)}$  values at various initial concentrations. Similar phenomenon was observed for the adsorption of  $Cu^{2+}$  onto MCFA [21]. Moreover, it can be seen that the values of the pseudo-second order rate constant decreased with the increasing initial concentration, whereas adsorption capacity,  $q_e$  values increased.

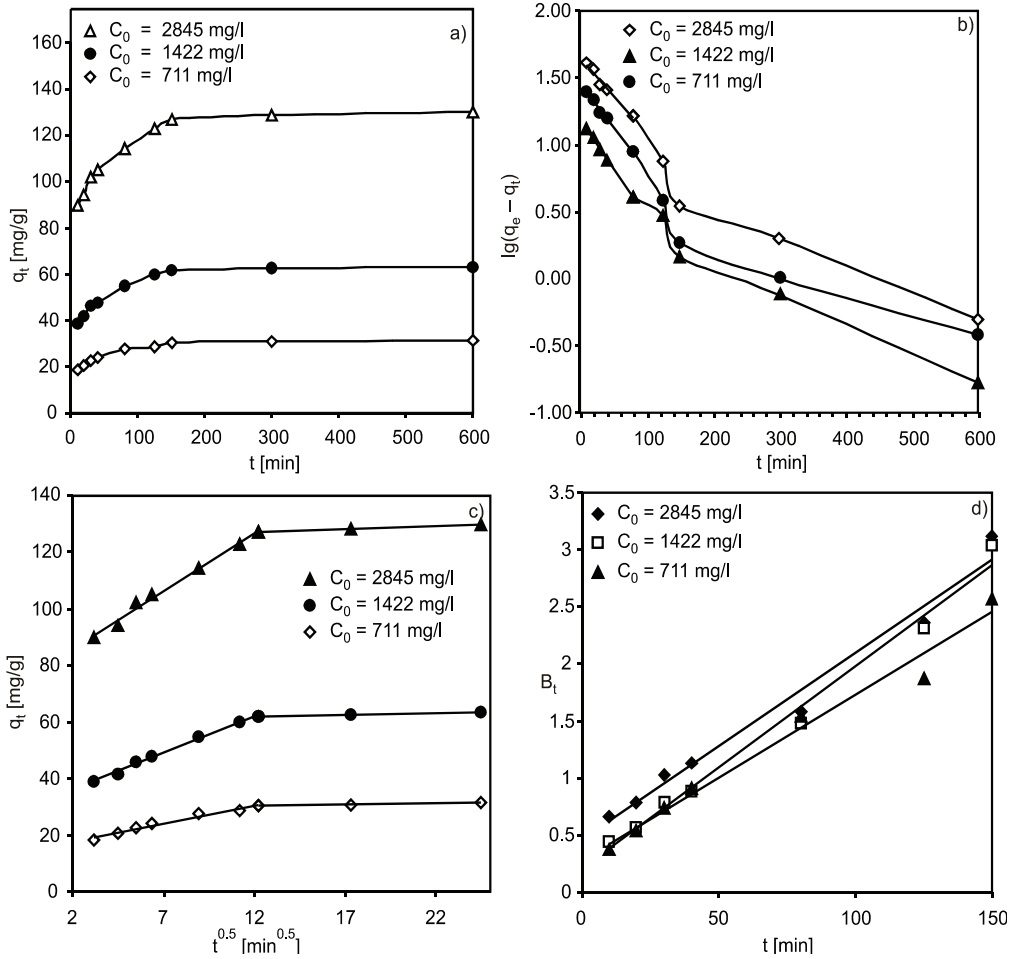


Fig. 6. Kinetics of OPs-CW adsorption onto MCFA ( $T = 303$  K,  $t = 10$  h, MCFA dosage = 2.0 g/l, pH = 6.0): a) effect of contact time, b) plot of pseudo-first order model, c) plot of Weber and Morris model, d) plot of Dumwald–Wagner model

The adsorption of OPs-CW onto MCFA is expected to proceed through the following sequence of steps: transport of OPs-CW from the boundary film to the external surface of the MCFA (film diffusion); transfer of OPs-CW from the surface to the intraparticle active sites (intraparticle diffusion); and uptake of OPs-CW by the active sites of MCFA (adsorption). Figure 6c shows the amount of COD adsorbed per unit weight of MCFA against square root of time by Weber and Morris model. It fits well in the two adsorption phases of 0–150 min ( $K_{\text{dif},1}$ ,  $C_1$ ) and 150–600 min ( $K_{\text{dif},2}$ ,  $C_2$ ). The data observed for the two phases of the reaction presents a good linearization in accordance with expected value by theory, indicating that intraparticle diffusion of OPs-CW onto MCFA is a rate controlling step. The constant  $C$  indicates that the resistance to

the external mass transfer increases as the intercept increases [22, 23]. We can see that  $C_1$  is significantly higher than  $C_2$ , this fact can be explained that the first phase is the diffusion of OPs-CW through the mesopore of MCFA. The second phase describes OPs-CW diffusion in micropores. The resistance of adsorbent in the mesopore diffusion is much lower than in the micropore. Moreover, the value of  $C$  increases with increasing initial OPs-CW concentration, which may be due to the greater driving force with increasing the initial concentration [24].

Table 2

Regression constants for pseudo-first order and pseudo-second order model of OPs-CW adsorption onto MCFA

$C_i$ [mg/l]	Pseudo-first order		Pseudo-second order				
	$K_1$ [1/min]	$R^2$	$q_{e(\text{calc})}$ [mg/g]	$K_2$ [g/(mg·min)]	$q_{e(\text{exp})}$ [mg/g]	$R^2$	$K_2 q_e^2$ [mg/g]
2845	0.0033	0.8973	131.58	0.0009	130.5	0.9999	15.8228
1422	0.0031	0.8462	64.52	0.0015	63.6	0.9999	6.1200
711	0.0032	0.9263	32.05	0.0027	31.665	0.9999	2.7293

Table 3

Regression constants for intraparticle diffusion model of OPs-CW adsorption onto MCFA

$C_i$ [mg/l]	Weber and Morris						Dumwald–Wagner	
	$K_1$ [mg/(g·min <sup>0.5</sup> )]	$C_1$ [mg/g]	$R^2$	$K_2$ [mg/(g·min <sup>0.5</sup> )]	$C_2$ [mg/g]	$R^2$	Intercept	$R^2$
2845	4.0579	77.867	0.9909	0.2426	124.13	0.9903	0.2035	0.9876
1422	2.5594	31.128	0.9936	0.1179	60.391	0.9676	0.459	0.978
711	1.261	15.197	0.9727	0.1047	28.968	0.9797	0.2791	0.9787

To further confirm the above results, in Fig. 6d dependences  $B_i(t)$  were plotted (the Dumwald–Wagner model,  $t < 150$  min).  $R^2$  were 0.9876, 0.978 and 0.9787 with respect to various initial COD concentrations, indicating that the result is consistent with the conclusions of the Weber–Morris model. However, for the Dumwald–Wagner model, if the linearity of the plots does not intersect the origin of coordinates, the rate limiting step is intraparticle diffusion process, otherwise that is film diffusion. Furthermore, the higher intercept indicates that film diffusion rate control step has greater influence on rate-limiting step [14]. From the intercepts shown in Table 2, we therefore can conclude that the rate-limiting step isn't a sole intraparticle diffusion process,, and there may also be film diffusion. The adsorption proceeds via a complex mechanism consisting of both film adsorption and intraparticle transport within the pores of MCFA.

## 3.5. ISOTHERM MODELING

Temperature has a pronounced effect on the adsorption capacity of the adsorbents. Figure 7a shows the equilibrium adsorption isotherm at various temperatures ranging from 303 K to 318 K for OPs-CW adsorption onto MCFA. In order to check which type of isotherm fits better the adsorption experimental data,  $C_e/q_e$  vs.  $C_e$  for Langmuir isotherm,  $\lg q_e$  vs.  $\lg C_e$  for Freundlich isotherm and  $\ln q_e$  vs.  $\varepsilon^2$  for D-R model were plotted (Figs. 7b–7d).

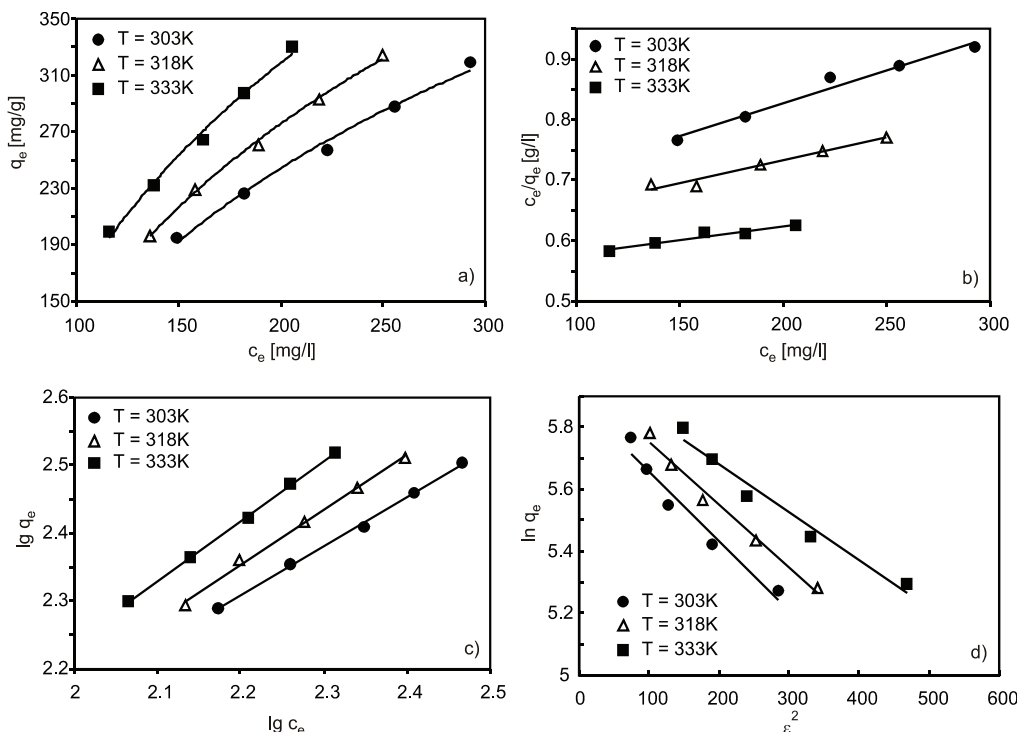


Fig. 7. Equilibrium isotherm of OPs-CW adsorption onto MCFA ( $T = 303$  K,  $t = 10$  h, MCFA dosage = 2 g/l, pH = 6.0): a) equilibrium adsorption isotherm, b) Langmuir model, c) Freundlich model, d) D-R model

The regression constants for all the models are listed in Table 4. The results showed that the adsorption was enhanced upon increasing temperature, suggesting that the adsorption process could be more likely chemical adsorption rather than physical one. The correlation coefficients ( $R^2 > 0.99$ ) was higher than that for the Langmuir model, which indicates that OPs-CW adsorption could be more well described by the Freundlich isotherm. The D-R model was also applied to estimate the porosity apparent free energy and the characteristics of adsorption. As an index of consumed energy

in adsorption,  $E_a$  presents the free energy per mole of adsorbent transferring from infinity in solution to the adsorbent surface. The value of  $E_a$  is lower than 8 kJ/mol suggests that the physical process dominates in adsorption. If the value of  $E_a$  is between 8 and 16 kJ/mol, the adsorption is of chemical nature [25]. The values of  $E_a$  calculated using Eqs. (11) were found to be 15.07, 15.81 and 16.67 kJ/mol for OPs-CW adsorption onto MCFA at 303, 318 and 333K, respectively. The  $R^2$  values are in the range of 0.9566–0.9842, indicating good performance of the D-R model. The values of  $E_a$  are estimated in the range of 8–16 kJ/mol, pointing that chemical bonding was referred to be the main adsorption mechanism, which will be further discussed by FT-IR technique.

Table 4

Langmuir, Freundlich and D-R isotherm model for OPs-CW adsorption onto MCFA

$T$ [K]	Langmuir			Freundlich			D-R isotherm			
	$q_0$ [mg/g]	$K_L$ [l/mg]	$R^2$	$K_F$ [l/mg]	$n$	$R^2$	$X'_m$ [mg/g]	$K'$ [mol <sup>2</sup> /kJ <sup>2</sup> ]	$E_a$ [kJ/mol]	$R^2$
303K	232.558	0.0020	0.9728	2.9751	1.1316	0.9992	105.4145	0.0022	15.0756	0.9566
318K	188.679	0.0038	0.9592	3.7549	1.2369	0.9962	77.1152	0.002	15.8114	0.9842
333K	166.667	0.0070	0.9398	5.2192	1.3829	0.9981	76.5237	0.0018	16.6667	0.969

FT-IR technique was used to examine the surface groups responsible for OPs-CW adsorption. The OPs-CW loaded MCFA samples were placed in an oven at 60 °C for 6 h. Figure 8 shows the FT-IR spectra of blank RCFA, blank MCFA and OPs-CW loaded MCFA.

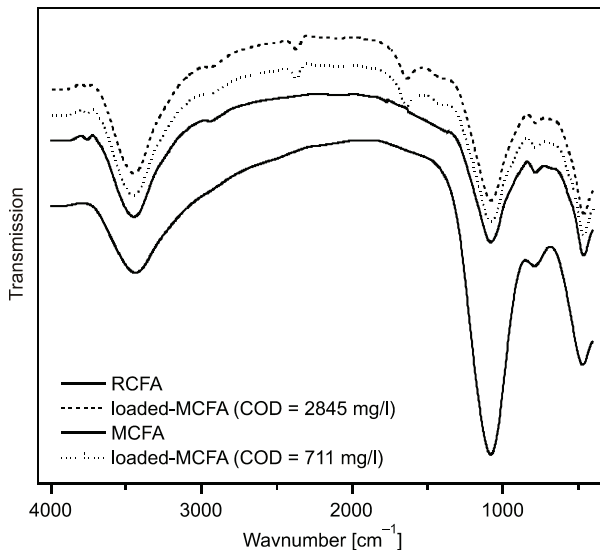


Fig. 8. FT-IR spectrogram of blank RCFA, MCFA and OPs-CW loaded MCFA

It is clear that there are no much difference between the RCFA and MCFA of FT-IR spectrogram. The FT-IR spectra of RCFA and MCFA show some fly ash characteristic absorption bands at  $3450\text{ cm}^{-1}$  and  $1082\text{ cm}^{-1}$  corresponding to the stretching vibration of O–H and bending vibration of Si–O, respectively [26]. However OPs-CW loaded MCFA displayed additional peaks around  $1660\text{ cm}^{-1}$  of aromatic ring skeleton vibration and around  $2372\text{ cm}^{-1}$  of C≡N stretching vibration compared with MCFA blank, these observations suggested attachments of cyanides and phenols from OPs-CW onto MCFA.

### 3.6. THERMODYNAMIC PARAMETERS

The plots of  $\ln K_d$  vs.  $1/T$  at initial COD concentrations are shown in Fig. 9. The thermodynamic parameters of  $\Delta H^\circ$  and  $\Delta S^\circ$  were calculated from the slope and intercept.

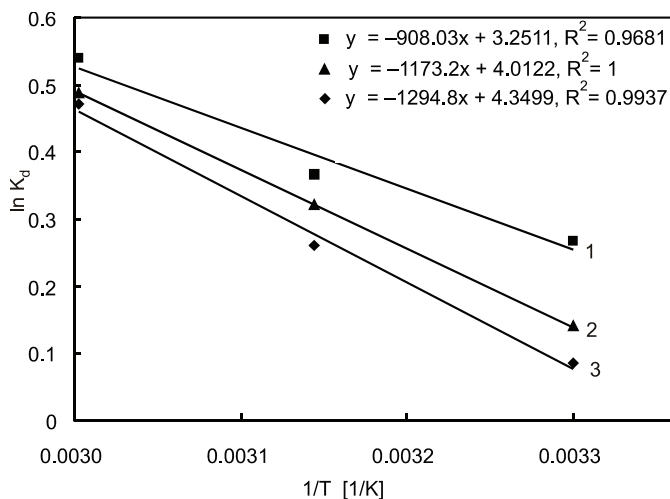


Fig. 9. The plot of  $\ln k_d$  vs.  $1/T$  at initial COD concentrations of 355 (1), 712 (2), and 2845 (3) mg/l of coking wastewater

The Gibbs free energies ( $\Delta G^\circ$ ) at various temperatures were calculated from Eqs. (12). The values of  $\Delta G^\circ$ ,  $\Delta H^\circ$ , and  $\Delta S^\circ$  for OPs-CW adsorption onto MCFA are shown in Table 5. At various temperatures and initial COD concentrations, the negative values of change in  $\Delta G^\circ$  demonstrate the feasibility and spontaneous nature of the adsorptive treatment, the enthalpy ( $\Delta H^\circ$ ) and entropy ( $\Delta S^\circ$ ) values were 17.549–20.765 kJ/mol and 27.03–36.165 J/(mol·K) under various initial OP-CWs, respectively, showing that the spontaneous reaction at high temperatures where exothermicity is relatively unimportant with randomness at the solid–solution interface during adsorption [27–31]. The adsorption energy is typically 5–10 kJ/mol for van der Waals forces between adsorbate and adsorbent, the chemisorption energy is generally, 30–70 kJ/mol for chemical bonds formed between molecules and the surface.

Table 5

Regression constants for thermodynamic parameters for the adsorption of OPs-CW onto MCFA

$C_i$ [mg/l]	$-\Delta G^\circ$ [kJ/mol]			$\Delta H^\circ$ [kJ/mol]	$\Delta S^\circ$ [J/(mol·K)]
	303 K	318 K	333 K		
355	2.675	2.925	3.358	17.549	27.03
712	2.354	2.812	3.233	19.754	33.357
2845	2.214	2.214	2.656	20.765	36.165

Therefore, the findings from this work strongly suggest that the adsorption system was spontaneous and endothermic in nature. The adsorption mechanism can be chemical adsorption with a chemical reaction or bond being involved in the adsorption process [24]. Strong dipole forces, hydrogen bonding and van der Waals forces played a major role [32, 33]. Similar findings were recorded by Nollet et al. in their work involving removal of HeCB using fly ash as an adsorbent [34]. The thermodynamic parameters for the adsorption of organic pollutants onto fly ash at various temperatures are summarized in Table 6.

Table 6

Thermodynamic parameters for the adsorption of organic pollutants onto fly ash

Adsorbent	Adsorbant	$T$ [K]	$-\Delta G^\circ$ [kJ/mol]	$\Delta H^\circ$ [kJ/mol]	$\Delta S^\circ$ [J/(mol·K)]	Reference
Bottom ash	Quinoline Yellow	293	7.2	50.8	112	[35]
		308	8.7			
		327	11.7			
Fly ash	Congo Red	303	20.8	27.1	118	[24]
		313	30.3			
		323	30.4			
Bagasse fly ash	Dairy wastewater	283	8.54	25.72	91.53	[7]
		293	9.79			
		303	10.35			
Fly ash	Anionic dyes	293	25.6	27.1	179.6	[11]
		313	25.4			

#### 4. CONCLUSIONS

The results of this work showed that the MCFA can be used as an effective adsorbent for the adsorption of OPs-CW. The following conclusions could be derived from the present study.

• Adsorption of OPs-CW onto MCFA was found to be dependent on the initial pH of solution and MCFA dosage. The results indicated that when the optimum dosage of MCFA was 2.0 g/l at the optimum pH of 6.0, 94.2% of COD removal could be achieved at 303K.

• The adsorption kinetics of OPs-CW onto MCFA was in agreement with the pseudo-second order model. The intraparticle diffusion was identified not to be a sole rate limiting step, there may also be film diffusion. The Freundlich equation well described the equilibrium adsorption. The values of  $E_a$  calculated by the D-R model are approximately in the range of 8–16 kJ/mol, which suggests that chemical bonding could be more likely the main adsorption mechanism. FTIR studies gave a further proof of the above conclusions.

• The thermodynamic adsorption parameters,  $\Delta H^\circ$  and  $\Delta S^\circ$  are 17.55–20.77 kJ/mol and 27.03–36.165 J/(mol·K) under various initial COD values and reaction temperatures, respectively. The findings from this work strongly suggest that the adsorption system was spontaneous and endothermic in nature.

#### ACKNOWLEDGEMENT

The author would like to thank the financial support from the Natural Science Research Project, Education Department, Anhui Province (Grant No. KJ2012A038).

#### REFERENCES

- [1] ZHANG M., TAY J.H., QIAN Y., GU X.S., *Water Res.*, 1998, 32 (2), 519.
- [2] KIM Y.M., PARK D., LEE D.S., PARK J.M., *J. Hazard. Mater.*, 1998, 152 (3), 915.
- [3] DĄBROWSKI A., PODKOŚCIELNY P., HUBICKI Z., BARCZAK M., *Chemosphere*, 2005, 58 (8), 1049.
- [4] DONALDSON F.P., NYMAN M.C., *Chemosphere*, 2006, 65 (5), 854.
- [5] QI R., YANG K., YU Z.-X., *J. Environ. Sci.*, 2007, 19 (2), 153.
- [6] ZHAO W.-T., HUANG X., LEE D.-J., *Sep. Purif. Technol.*, 2009, 66 (2), 279.
- [7] KUSHWAHA J.P., SRIVASTAVA V.C., MALL I.D., *Bioresour. Technol.*, 2010, 101 (10), 3474.
- [8] PAPANDEOU A., STOURNARAS C.J., PANIAS D., *Copper and cadmium adsorption on pellets made from fired coal fly ash*, *J. Hazard. Mater.*, 2007, 148 (3), 538.
- [9] WANG S.-B., MA Q., ZHU Z.H., 2008, 87 (15–16), 3469.
- [10] NASCIMENTO M., MOREIRA SOARES P.S., DE SOUZA V.P., *Fuel*, 2009, 88 (9), 1714.
- [11] SUN D., ZHANG X., WU Y., LIU X., *J. Hazard. Mater.*, 2010, 181, 335.
- [12] APHA, *Standard methods for the examination of water and wastewater*, 20th ed., American Public Health Association, Washington, DC, USA, 1998.
- [13] WEBER W.J., MORRIS J.C., *J. Sanitary Eng. Div. Proceed Am. Soc. Civil Eng.*, 1963, 89, 31.
- [14] BOYD G.E., ADAMSON A.W., MYERS L.S., *J. Am. Chem. Soc.*, 1947, 69 (11), 2836.
- [15] MALL I.D., SRIVASTAVA V.C., AGARWAL N.K., *Dyes Pigments*, 2006, 69 (3), 210.
- [16] GUPTA V.K., MITTAL A., GAJBE V., *J. Colloid Interf. Sci.*, 2005, 284 (1), 89.
- [17] BRUNAUER S., EMMETT P.H., TELLER E., *J. Amer. Chem. Soc.*, 1938, 60, 309.
- [18] BARRETT E.P., JOYNER L.G., HALENDA P.P., *J. Am. Chem. Soc.*, 1951, 73, 373.
- [19] BENNY T.H., BANDOSZ T.J., WONG S.S., *J. Colloid Interface Sci.*, 2008, 317 (2), 375.

- 
- [20] EL-NAAS M.H., AL-ZUHAIR S., ALHAIJA M.A., *J. Hazard. Mater.*, 2010, 173, 750.
- [21] HSU T.-C., YU C.-C., YEH C.-M., *Fuel*, 2008, 87 (7), 1355.
- [22] MCKAY G., OTTERBURN M.S., AGA J.A., *Water Air Soil Poll.*, 1985, 24 (3), 307.
- [23] ACEMIOĞLU B., *J. Colloid. Interf. Sci.*, 2004, 274 (2), 371.
- [24] AKSU Z., KABASAKAL E., *Sep. Purif. Technol.*, 2004, 35 (3), 223.
- [25] HO Y.-S., PORTER J.-F., MCKAY G., *Water Air Soil Pollut.*, 2002, 141, 1.
- [26] S. Deng, R. Bai, J.P. Chen, *J. Colloid Interf. Sci.*, 2003, 260 (2), 265.
- [27] ÖZCAN A., SAFA ÖZCAN A., TUNALI S., AKAR T., KIRAN I., *J. Hazard. Mater.*, 2005, 124 (1–3), 200.
- [28] SAG Y., KUTSAL T., *Biochem. Eng. J.*, 2000, 6 (2), 145.
- [29] GUPTA V.K., ALI I., *J. Colloid Interf. Sci.*, 2004, 271 (2), 321.
- [30] OPEN B.V., KORDE W. L., KLEIN W., *Chemosphere*, 1991, 22, 285.
- [31] NAMASIVAYAM C., RANGANATHAN K., *Water Res.*, 1995, 29 (7), 1737.
- [32] OPEN B.V., KÖRDEL W., KLEIN W., *Chemosphere*, 1991, 22, 285.
- [33] CHIOU C.T., KILE D.E., *Environ. Sci. Technol.* 1994, 28, 1139.
- [34] NOLLET H., ROELS M., LUTGEN P., DER-MEEREN P.V., VERSTRAETE W., *Chemosphere*, 2003, 53 (6), 655.
- [35] GUPTA V.K., MITTAL A., GAJBE V., *J. Colloid Interf. Sci.*, 2005, 284 (1), 89.